



## Pressure drop in two phase slug/bubble flows in mini scale capillaries

Ed Walsh<sup>a,\*</sup>, Yuri Muzychka<sup>b,c,1</sup>, Patrick Walsh<sup>a</sup>, Vanessa Egan<sup>a</sup>, Jeff Punch<sup>b</sup>

<sup>a</sup>Stokes Institute, Mechanical & Aeronautical Engineering Dept., University of Limerick, Ireland

<sup>b</sup>CTVR, Stokes Institute, Mechanical & Aeronautical Engineering Dept. University of Limerick, Ireland

<sup>c</sup>Faculty of Engineering and Applied Science, Memorial University of Newfoundland, St. John's, NL, Canada A1B 3X5

### ARTICLE INFO

#### Article history:

Received 1 May 2009

Received in revised form 27 June 2009

Accepted 29 June 2009

Available online 5 July 2009

#### Keywords:

Taylor flow

Plug flow

Segmented flow

Pressure drop

Bio-fluidics

Micro-channels

### ABSTRACT

A segmented two phase slug/bubble flow occurs where a liquid and a gas are pumped into the same tube over a range of Reynolds numbers. This segmented two phase flow regime is accompanied by an increase in pressure drop relative to the single phase flow where only one fluid is flowing in a capillary. This work experimentally and theoretically examines the pressure drop encountered by the slug/bubble flow with varying slug lengths in mini channels. In the experimental work the dimensionless parameters of Reynolds number and Capillary number span over three orders of magnitude, and dimensionless slug length ranges over two orders of magnitude to represent flows typical of mini- and micro-scale systems. It is found, in agreement with previous work, that these dimensionless groups provide the correct scaling to represent the pressure drop in two phase slug/bubble flow, although the additional pressure drop caused by the interface regions was found to be ~40% less than previously reported.

© 2009 Elsevier Ltd. All rights reserved.

### 1. Introduction

Many different regimes of two phase flow have been studied from pressure drop, mass transfer and heat transfer perspectives, and are typically characterized by the terminology of bubbly, slug, mist, annular, wavy or stratified flow regimes. Many authors have formulated charts in an attempt to identify which type of flow regime is most likely under defined gas and liquid flow rates without giving much consideration to the local flow-field. For example, in the slug flow regime the actual length of the slugs is not typically measured although it was shown, some time ago, to be important on the resultant pressure drop, mass and heat transfer by Horvath et al. (1973). A two phase non-boiling slug flow regime is the focus of the current study and a diagrammatic sketch is shown in Fig. 1, where a gaseous flow is used to segment a continuous liquid stream, to create a well ordered train of segmented slugs. This two phase flow can provide significant heat transfer improvements over low profile single phase systems such as those studied by Walsh et al. (2008), Walsh and Grimes (2007), Egan et al. (2009a,b).

As seen from this figure a large number of different configurations are possible for the same gas and liquid flow rates depending

on the ratio of slug length to channel diameter ( $L_s/d$ ). These non-boiling slug flows are commonly found in many industrial applications such as monoliths catalyst structures (Kreutzer et al., 2005), petroleum industry (Lin and Tavlarides, 2009; Kim and Ghajar, 2002), micro-fluidic biological processing (Gunther et al., 2004; Walsh et al., 2006, 2007; King et al., 2007) and micro-reactors (Waelchli and von Rohr, 2006). The latter resulting in bio-compatibility issues between the two phases employed (Walsh et al., 2005).

In recent works by the authors, we report new experimental data, which considers the slug/bubble lengths, for two phase slug flows in circular tubes with a constant heat flux boundary condition (Walsh et al., 2009), and developed a model which addresses the effect of slug length on Nusselt number (Muzychka et al., 2009). The present work addressed the pressure drop encountered by the slug/bubble flow with varying slug lengths in mini channels. The present model, in conjunction with proper heat and mass transfer models, allows for concise design and analysis of slug flow systems for a wide range of applications, such as those noted above.

Pressure drop in such systems is a key parameter in terms of, flow rates, stability of parallel channel, sizing of pumps and overall design of any two phase system. The simplest approach to modelling two phase flows is the separated flow model, which considers both phases independently and predicts the resultant pressure drop to be the sum of their single phase contributions. This model does not account for any additional pressure drop associated with the interfaces between the two phases. In an attempt to account for this additional interfacial pressure drop, Lockhart and Martinelli (1949) extended the separated flow model to include an empirical

\* Corresponding author. Tel.: +353 61 213181; fax: +353 61 202393.

E-mail addresses: [edmond.walsh@ul.ie](mailto:edmond.walsh@ul.ie) (E. Walsh), [y.s.muzychka@gmail.com](mailto:y.s.muzychka@gmail.com) (Y. Muzychka), [pat.walsh@ul.ie](mailto:pat.walsh@ul.ie) (P. Walsh), [Vanessa.egan@ul.ie](mailto:Vanessa.egan@ul.ie) (V. Egan), [jeff.punch@ul.ie](mailto:jeff.punch@ul.ie) (J. Punch).

<sup>1</sup> Sabbatical address: Stokes Institute, Mechanical and Aeronautical Engineering Department, University of Limerick, Ireland.

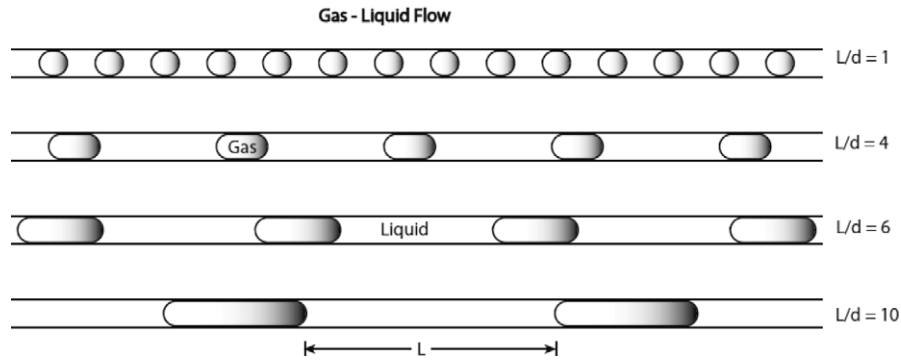


Fig. 1. Gas–liquid slug flow with varying slug lengths for constant flow rates.

parameter to account for the interfacial effects. The empirical parameter seeks to provide a solution for most types of two phase flows, bubbly, mist, annular, wavy or stratified flow regimes, and does not distinguish between the different physics associated with different flow regime. Hence, while the general applicability of the model without specific knowledge of the flow patterns is one of the reasons for its widespread use, the resultant interfacial pressure drop predictions are an order of magnitude estimate, which is not typically acceptable for environments such as chemical processing or lab on chip applications. Moreover, despite their original paper specifically stating that the model cannot be applied to slug flows many authors continue to use it with some reasonable results; however, it will not be considered any further in this paper as it lacks any physics of the problem. For completeness the data are presented using separated flow models and the results are shown in the [Electronic annex](#) to this paper.

This paper is focussed upon the segmented slug/bubble flow regime of Fig. 1, where liquid slugs and gas bubbles are transported through a circular capillary. Five different liquids with a Reynolds number and Capillary number range of several orders of magnitude are examined and appropriate scaling is demonstrated to collapse the data. The asymptotic limits of many slugs and few slugs illustrates the range in which it is necessary to consider the pressure drop contribution from the gas/bubble interface region and Poiseuille flow region of the non-boiling two phase slug flows.

## 2. Theory

The pressure drop in fully developed laminar tube flow is given by

$$\frac{\Delta P}{L} = \frac{16}{Re} \left( \frac{1}{2} \rho U^2 \right) \frac{4}{d} \quad \text{or more concisely } fRe = 16 \quad (1)$$

where  $\Delta P$ ,  $LRe$ ,  $\rho$ ,  $U$ ,  $d$  and  $f$  are the pressure drop, length of the capillary, Reynolds number, density, mean velocity of the fluid, tube diameter and friction factor, respectively. The introduction of a second phase to create a segmented bubble flow results in an increase in the pressure drop over the single phase case. Hence the total pressure drop in a tube can be expressed as the sum of, the single phase pressure drop, and the additional pressure drop caused by the presence of the bubbles of air as

$$\Delta P_t = \Delta P_s + \Delta P_b \quad (2)$$

where the subscripts  $t$ ,  $s$  and  $b$  refer to the total, single phase and bubble related pressure drops. These equations combine to yield the total pressure drop in a segmented two phase flow as

$$fRe_t = 16 + \frac{\Delta P_b^*}{2L^*} \quad (3)$$

$$\text{where } \Delta P_b^* = \frac{\Delta P_b d}{\mu U}; L^* = \frac{L_s}{d}$$

where  $L_s$  and  $\mu$  are the length of the liquid slugs and the dynamic viscosity of the liquid. The term,  $\frac{\Delta P_b^*}{2L^*}$ , represents the pressure drop due to the addition of gas bubbles to the flow. The problem now turns to determination of  $\Delta P_b^*$ . Bretherton (1961) developed a theoretical solution for the pressure drop caused by a single bubble in two phase flows, where he corrected for the change in curvature due to the film surrounding the bubble, and accounted for the Laplace pressure term and change in film thickness to yield

$$\Delta P_b = 7.16(3Ca)^{\frac{2}{3}} \frac{\sigma}{d} \quad (4)$$

where  $\sigma$  is the interfacial tension between the liquid and the gas. This equation was derived for horizontal tubes under the assumption that the film thickness,  $\delta$ , was much less than the tube radius,  $r$ . Substitution of Bretherton (1961) result for pressure drop into Eq. (4) results in the pressure drop described as a function of Capillary number and slug length, only, to give

$$fRe = 16 + \frac{7.16(3Ca)^{\frac{2}{3}}}{2L^*Ca} \quad (5)$$

The assumption that the film thickness is small compared to the tube radius has been shown to be invalid at Reynolds numbers of order 100. Also the flow structure around the bubble, and hence pressure drop is influence by Reynolds number and therefore bubble pressure drop can be expected to be a function of  $Re$ ,  $Ca$  and  $L^*$  rather than simply  $Ca$ . Several authors (Aussillous and Quere, 2000; Grimes et al., 2007) have also found that the film thickness predicted by the theoretical solution of Bretherton (1961) does not agree well with experiments at both high and low Capillary numbers.

## 3. Experimental details and facility

A two phase flow was created using simple tee junctions of different diameters connected to separate syringe pumps to control the flow rate of both phases. Separate syringe pumps allowed the relative flow rates, and hence slug and bubble lengths to be varied over a wide range. The pressure drop was measured in hard walled capillaries, stainless steel and PFA Teflon, with a nominal internal diameter of 1 mm, with tube lengths between pressure tapings ranging from 1 to 2 m depending on the pressure range for each liquid used. Three pressure transducers, manufacturer's accuracy of 0.1% of the full scale deflection, with a range of 14 kPa, 35 kPa and 75 kPa were used to allow for the large range in pressure drop associated with the liquids of different viscosities. The experimental arrangement is shown in Fig. 2. The time required to reach steady state varied considerably over the range of liquids used, typically 10 min for the low viscosity liquids and up to half an hour for the high viscosity liquids. Due to this long settling period it proved necessary to connect the output from the pressure

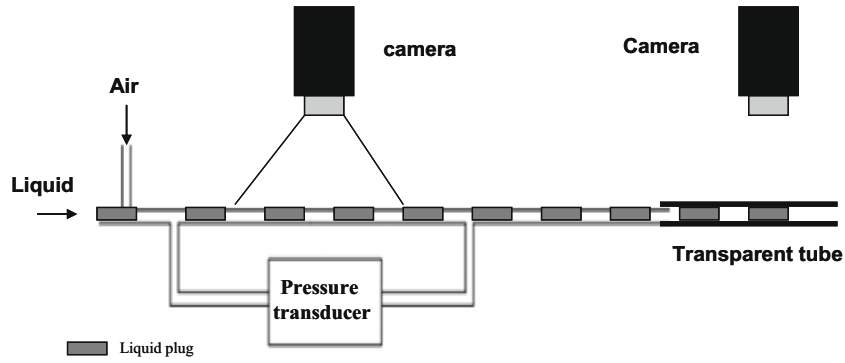


Fig. 2. Pressure drop measurement facility, liquid and air supply from syringe pumps and camera position movable depending on the tube material used.

transducer to a PC to monitor the pressure variation over time and identify when a steady state was achieved. The liquid was collected in a reservoir at the exit of the capillary where its temperature was measured using a K-type probe.

The pressure drop for single phase fully developed flow in a circular tube is given by Eq. (6). The lowest  $x/dRe_d$  value employed in these tests was 3, which ensures that the entrance length effects can be neglected as they account for less than 1% of the total pressure drop. Here,  $x$  is the distance from the inlet. From Eq. (6) the pressure drop is inversely proportional to the radius to the power of four and hence small errors in the radii can result in large errors in the calculated friction factor. The capillary manufacturers typically provide an uncertainty of up to 50  $\mu\text{m}$  of the nominal diameter of each capillary. To determine the diameter of the tube more accurately, a liquid with known viscosity, in this case water, was passed through each tube at a range of flow rates. This allowed the radius of each tube to be specified accurately.

$$\Delta P = \frac{8\mu L Q}{\pi R^4} \quad (6)$$

After the correct diameter was determined the viscosity of each liquid could be measured directly, again through Eq. (6). The measurements of both diameter and viscosities agreed reasonably well with the manufacturer's tolerances and data sheets, although it should be noted that *n*-alkane liquids have a large variation in viscosity with small changes in temperature. For example, the dynamic viscosity of FC40 varies by ~25% over a temperature range of 15–25 °C which could be a typical range in any laboratory environment.

The slug/bubble length was found to be a key variable in these experiments and hence it was necessary to ensure that a consistent slug train was created, which did not break down in the capillary. This was monitored using a camera in the test section, for the transparent PFA capillary and at the exit of the stainless steel capillary where the bubbles entered transparent tubing. A sample image of air bubbles in a liquid is shown in Fig. 3. The length of the slugs and bubbles were measured for each test using a number of camera images and a custom programme to obtain the average lengths for each experimental pressure drop recorded. It was noted that the slug length varied by ~10% for the measurements herein.

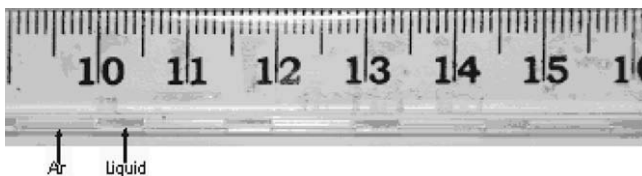


Fig. 3. Typical images used to deduce slug length within capillaries.

Table 1  
Range of dimensionless experimental parameters considered in this study.

Liquid	Re	Ca	Bond	Ca/Re	$L^*$
Water	255–1024	0.0033–0.0133	0.034	0.000013	21–102
FC40	11–86	0.006–0.05	0.28	0.000586	3–26
Dodecane	54–209	0.0067–0.026	0.08	0.000123	2.3–48
AR 20 Si oil	1.58–10	0.034–0.2	0.12	0.019	1.9–36
<i>n</i> -Hexane	358–956	0.0023–0.006	0.1	0.0000064	3–60

In all experiments air was used as the gas, while water, FC40, dodecane, AR 20 silicone oil and *n*-hexane were used as the liquid phases. Table 1 summarises the resultant range of dimensionless parameters of the experiments in this study. Importantly, the bond number is much less than one and hence the effects of gravity are not considered important in the measurement region. The Reynolds and Capillary numbers span over three orders of magnitude, and the dimensionless slug length ranges over two orders of magnitude. These ranges are expected to reflect the range of dimensionless parameters seen in micro- to mini-scale fluidic systems.

#### 4. Results and discussion

Fig. 4 shows images taken for liquid/air combinations in the PFA tubing, from the minimum to maximum superficial velocity for each liquid. It is seen that the meniscus changes with velocity on the leading and trailing edges of the bubbles. This is particularly evident from the *n*-hexane images where for the minimum velocity

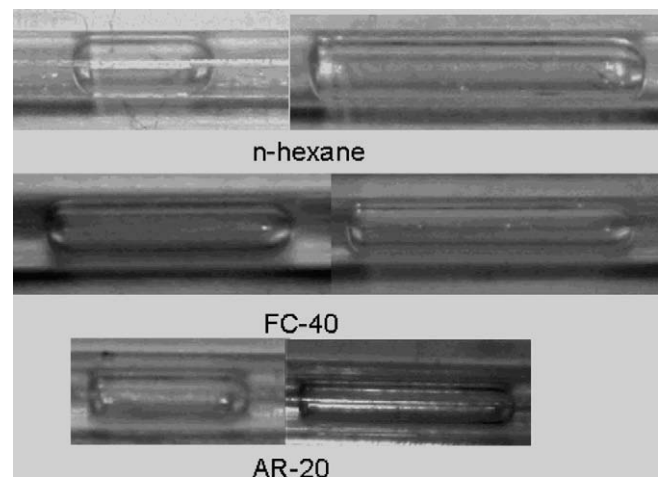


Fig. 4. Bubble flowing from left to right in transparent tubes at minimum (left) and maximum (right) velocities of the measured range.

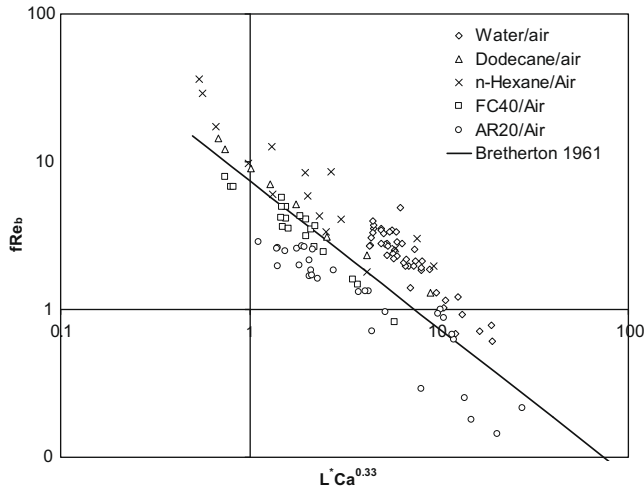


Fig. 5. Non-dimensional bubble pressure drop ( $fRe_b$ ) compared with the theoretical solution of Bretherton (1961) using Eq. (5).

the rear of bubble has a strong convex curvature, while at the higher velocity it has become almost flat.

All of the measured pressure data are presented in Fig. 5, along with the theoretical result of Bretherton (1961), Eq. (5) interfacial contribution. Although the Bretherton (1961) theory appears to broadly agree with the data, there is a high level of scatter. It is clear that  $Ca$  and  $L^*$  result in a poor correlation over the range of measurements.

From simulations at  $Re = 1$  of Kreutzer et al. (2005) (their Fig. 4), they found that at low  $Ca$  the simulation resulted in a slightly higher pressure drop than the theory, and at high  $Ca$  the reverse was found. Fig. 6 shows the same data as Fig. 5 but now scaled using  $(Ca/Re)^{0.33}$ . The best fit to the data takes the form of

$$fRe = \underbrace{16}_{\text{Single phase}} + \underbrace{\frac{\alpha}{L^*} \left(\frac{Re}{Ca}\right)^\beta}_{\text{Interfacial}} \quad (7)$$

where  $\alpha = 1.92$  and  $\beta = 0.33$ . Eq. (7) represents a linear superposition of the single phase Poiseuille flow and an empirically derived interfacial or Taylor flow limit. Transition from Poiseuille

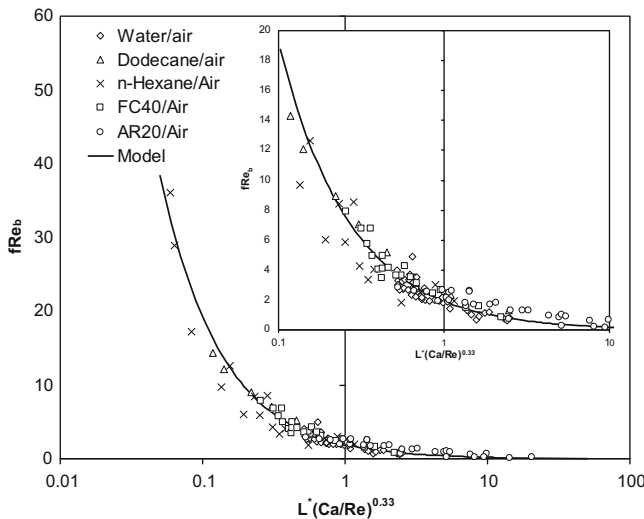


Fig. 6. Non-dimensional bubble pressure drop. Inset shows degree of scatter in low  $fRe_b$  range.

dominated flow to Taylor dominated flow occurs when both terms contribute equally in an order of magnitude sense or when:

$$\underbrace{16}_{\text{Poiseuille flow}} \sim \underbrace{\frac{\alpha}{L^*} \left(\frac{Re}{Ca}\right)^\beta}_{\text{Taylor flow}} \quad (8)$$

$$L^* \left(\frac{Ca}{Re}\right)^{0.33} \sim \left(\frac{1.92}{16}\right) \sim 0.1 \quad (9)$$

Thus when  $L^*(Ca/Re)^{0.33} \gg 0.1$ , the effect of slug length is not significant and the pressure drop in the flow is dominated by the characteristically Poiseuille flow, while for  $L^*(Ca/Re)^{0.33} \ll 0.1$  the effect of slugs is significant and the pressure drop in the flow is characteristically Taylor flow. This intersection of asymptotes approach is illustrated in Fig. 7 with the measured data. The region where the current measurements fall is in the region where both asymptotes provide a significant contribution to the total pressure drop. Hence the contribution from both asymptotes will usually be of interest in practical applications.

The constant,  $\alpha$ , was stated to be 2.72 by Kreutzer et al. (2005) from experimental data for Reynolds and Capillary numbers in the range of 150–1400 and 0.0027–0.04, respectively, in a 2.3 mm diameter tube. However, based on simulations they found a constant of  $\alpha = 1.12$  for  $Re > 50$ . From our measurements the determined constant is approximately the average of the simulation and correlated values of Kreutzer, additionally the low Reynolds number data agree quite well with all the other data sets, albeit a slightly higher constant would fit them better. At any rate, Kreutzer et al. (2005) suggest that the differences between their measurements and experiments are due to a Marangoni effect as a result of impurities in the liquids used. The effect of the impurities is to change the liquid gas interface between the limits of a no-shear and no-slip boundary condition. As shown originally by Bretherton (1961), this can change the pressure drop over a bubble by a factor of 2.5, further detailed by Ratulowski and Chang (1990). However, this explanation seems unlikely to be the cause of the difference in the constant,  $\alpha$ , as it would require enough surfactant in each case to result in the no-slip boundary condition. King et al. (2007), using particle image velocimetry, have shown the no-slip,

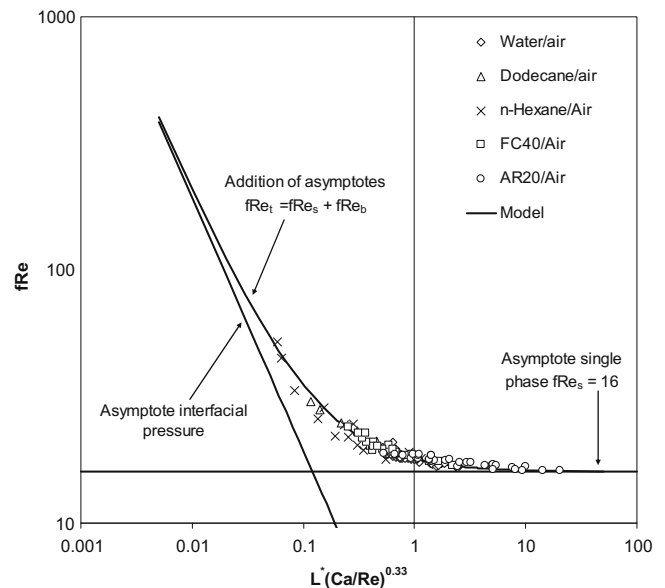


Fig. 7. Intersection of asymptotes approach to slug/bubble flows demonstrating regions where both the single phase and interfacial pressure asymptotes dominate the total pressure drop.

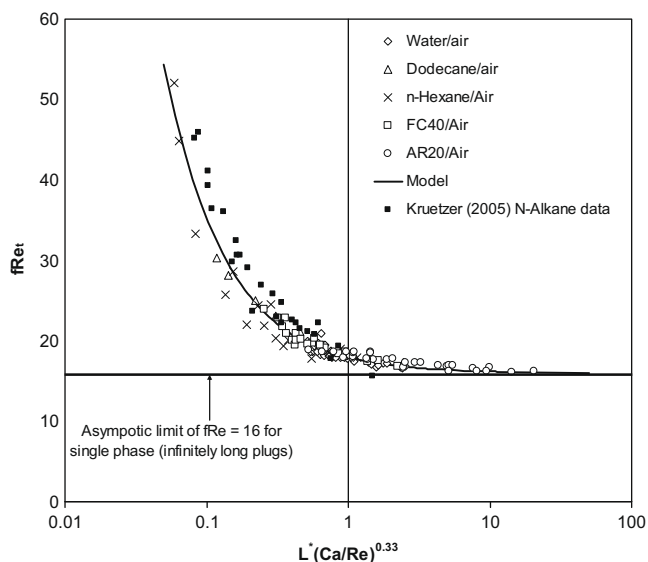


Fig. 8. Non-dimensional total pressure drop with the data of Kretzner et al. (2005) for *n*-alkanes included with a modified viscosity.

or no-shear, boundary condition is also a function of slug length and velocity in two immiscible liquid phases in a micro-channel by measuring the flow-field within the slugs (defined as the liquid that did not make contact with the wall, similar to the gas bubbles here). They found the flow-field within a slug could be either completely stagnant, or assume a full developed Hagen Poiseuille velocity profile, depending on both the length and velocity of the slugs. Importantly, they shunted the same slug back and forth, and hence any issues associated with impurities of the liquids were constant. A possibility is that the distribution of impurities can vary with the strength of the circulation with a bubble. A point worth noting is that Kretzner et al. (2005) state that  $\alpha = 2.72$ , however, the curve fit that they present as the best fit to their experimental data in Fig. 14 results in  $\alpha \sim 3.52$ , the reason for this substantial difference is unknown and no explanation is provided.

The total  $fRe$  of Kretzner et al. (2005) for the *n*-alkane liquids is plotted in Fig. 8 with the current data, where the viscosity of the Kretzner data is reduced by 10%, and shows reasonable agreement with the current measurements. This level of viscosity change would only require a 5 K change in liquid temperature using the equations of Dymond and Oye (1994). Kretzner et al. (2005) does not report any temperature measurement in their experiments, and simply report the physical properties of the liquids at 293 K, hence it is feasible that the variation of viscosity due to temperature of the *n*-alkane liquids could explain the differences in the measurement of Kretzner et al. (2005) and herein. The new experimental data in tabulated form is available in the Electronic annex of this paper for future use by others.

Finally, all of these models assume that a thin film exists between the air bubble and the wall which results in the bubble leading edge having a convex shape as demonstrated in Fig. 4. The terms, wet and dry wall have been used by Lee and Lee (2008) to differentiate between flows where a liquid film is present and is not. The latter would be in direct contradiction to the assumptions of the theory of Bretherton (1961) and hence cannot be expected to predict such flow regimes. Lee and Lee (2008) have shown that the pressure drop in the case of a dry wall, as found using water/air in a Teflon tube resulted in significantly higher pressure drop due to increased contact angles; and the models of Chisholm (1967) failed to represent the experimental measurements within the usual bounds. Hence

determination of the pressure drop in a segmented flow not only requires knowledge of slug length, but also the behaviour between the capillary material and fluids employed.

## 5. Conclusions

This work confirms the scaling group in a model for the prediction of pressure drop in slug/bubble segmented flows as a function of  $L^*$  and  $Ca/Re$ , and demonstrates the theory of Bretherton is found lacking. The results showed good agreement across a wide range of Reynolds and Capillary numbers using these scaling parameter. The scaling used can be represented by two asymptotes to represent the conditions of few slugs and many slugs, the range where both asymptotes contributed significantly to the total pressure drop was also confirmed as a function of  $L^*(Ca/Re)^{0.33}$  and found to be of order  $\sim 0.1$ .

## Acknowledgements

The authors acknowledge the financial support of Science Foundation Ireland under Grant No. 03/CE3/I405 and of Enterprise Ireland.

## Appendix A. Supplementary data

Supplementary data associated with this article can be found, in the online version, at doi:10.1016/j.ijmultiphaseflow.2009.06.007.

## References

- Aussillous, P., Quere, D., 2000. Quick deposition of a fluid on the wall of a tube. *Phys. Fluids* 12, 2367–2371.
- Bretherton, F.P., 1961. The motion of long bubbles in tubes. *J. Fluid Mech.* 10, 166–188.
- Chisholm, D., 1967. A theoretical basis for Lockhart–Martinelli correlation for 2-phase flow. *Int. J. Heat Mass Transfer* 10, 1767–1778.
- Dymond, J.H., Oye, H.A., 1994. Viscosity of selected liquid *n*-alkanes. *J. Phys. Chem. Ref. Data* 23, 41–53.
- Egan, V., Stafford, J., Walsh, P., Walsh, E., Grimes, R., 2009a. An experimental study on the performance of miniature heat sinks for forced convection air cooling. *ASME J. Heat Transfer* 130.
- Egan, V., Walsh, P., Walsh, E., Grimes, R., 2009b. A novel heat sink design for cooling of low profile electronic devices. *ASME J. Elec. Pack.* 131.
- Grimes, R., King, C., Walsh, E., 2007. Film thickness for two phase flow in a microchannel. *Adv. Appl. Fluid Mech.* 2, 59–70.
- Gunther, A., Khan, S.A., Thalmann, M., Trachsel, F., Jensen, K.F., 2004. Transport and reaction in microscale segmented gas–liquid flow. *Lab Chip* 4, 278–286.
- Horvath, C., Solomon, B.A., Engasser, J.M., 1973. Measurement of radial transport in slug flow using enzyme tubes. *Ind. Eng. Chem. Fund.* 12, 431–439.
- Kim, D., Ghajar, A., 2002. Heat transfer measurements and correlations for air–water flow of different flow patterns in a horizontal pipe. *Exp. Therm. Fluid Sci.* 25, 659–676.
- King, C., Walsh, E., Grimes, R., 2007. PIV measurements of flow within plugs in a microchannel. *Microfluid. Nanofluid.* 3, 463–472.
- Kretzner, M.T., Kapteijn, F., Moulijn, J.A., Kleijn, C.R., Heiszwolf, J.J., 2005. Inertial and interfacial effects on pressure drop of Taylor flow in capillaries. *AIChE J.* 51, 2428–2440.
- Lee, C.Y., Lee, S.Y., 2008. Pressure drop of two-phase plug flow in round mini-channels: influence of surface wettability. *Exp. Therm. Fluid Sci.* 32, 1716–1722.
- Lin, R., Tavlarides, L.L., 2009. Flow patterns of *n*-hexadecane–CO<sub>2</sub> liquid–liquid two-phase flow in vertical pipes under high pressure. *Int. J. Multiphase Flow* 35, 566–579.
- Lockhart, R.W., Martinelli, R.C., 1949. Proposed correlation of data for isothermal 2-phase, 2-component flow in pipes. *Chem. Eng. Prog.* 45, 39–48.
- Muzychka, Y.S., Walsh, E.J., Walsh, P., 2009. Heat transfer enhancement using laminar gas–liquid segmented fluid streams. *InterPak 2009*, San Francisco, USA.
- Ratulowski, J., Chang, H.C., 1990. Marangoni effects of trace impurities on the motion of long gas-bubbles in capillaries. *J. Fluid Mech.* 210, 303–328.
- Waelchli, S., von Rohr, P.R., 2006. Two-phase flow characteristics in gas–liquid microreactors. *Int. J. Multiphase Flow* 32, 791–806.
- Walsh, E., Grimes, R., 2007. Low profile fan and heat sink thermal management solution for portable applications. *Int. J. Therm. Sci.* 46, 1182–1190.
- Walsh, E.J., King, C., Grimes, R., Gonzalez, A., 2005. Segmenting fluid effect on PCR reactions in microfluidic platforms. *Biomed. Microdevices* 7, 269–272.

- Walsh, E.J., King, C., Grimes, R., Gonzalez, A., 2006. Influence of segmenting fluids on efficiency, crossing point and fluorescence level in real time quantitative PCR. *Biomed. Microdevices* 8, 59–64.
- Walsh, E.J., King, C., Grimes, R., Gonzalez, A., Ciobanu, D., 2007. Compatibility of segmenting fluids in continuous-flow microfluidic PCR. *J. Med. Devices* 1, 241–245.
- Walsh, E.J., Walsh, P., Grimes, R., Egan, V., 2008. Thermal management of low profile electronic equipment using radial fans and heat sinks. *ASME J. Heat Transfer* 130.
- Walsh, P.A., Walsh, E.J., Muzychka, Y.S., 2009. Laminar slug flow-heat transfer characteristics with constant heat flux boundary. In: *Proceedings of the HT2009 2009 ASME Summer Heat Transfer Conference, San Francisco, USA*.